THE JOURNAL OF BIOLOGICAL CHEMISTRY VOL. 281, NO. 42, pp. 31326–31336, October 20, 2006

The Tail Domain of Myosin Va Modulates Actin Binding to One Head*[S]

Received for publication, April 24, 2006, and in revised form, August 10, 2006 Published, JBC Papers in Press, August 18, 2006, DOI 10.1074/jbc.M603898200

Adrian O. Olivares[‡1], **Wakam Chang**[§], **Mark S. Mooseker**[§¶], **David D. Hackney**[‖], **and Enrique M. De La Cruz**[‡2]

From the Departments of [‡]*Molecular Biophysics and Biochemistry,* [§]*Cell Biology, and* [¶]*Molecular, Cellular, and Developmental Biology and Pathology, Yale University, New Haven, Connecticut 06520 and the* [‖]*Department of Biological Sciences, Carnegie Mellon University, Pittsburgh, Pennsylvania 15213*

Calcium activates full-length myosin Va steady-state enzymatic activity and favors the transition from a compact, folded "off" state to an extended "on" state. However, little is known of how a head-tail interaction alters the individual actin and nucleotide binding rate and equilibrium constants of the ATPase cycle. We measured the effect of calcium on nucleotide and actin filament binding to full-length myosin Va purified from chick brains. Both heads of nucleotide-free myosin Va bind actin strongly, independent of calcium. In the absence of calcium, bound ADP weakens the affinity of one head for actin filaments at equilibrium and upon initial encounter. The addition of calcium allows both heads of myosin Va·ADP to bind actin strongly. Calcium accelerates ADP binding to actomyosin independent of the tail but minimally affects ATP binding. Although ^{18}O exchange and product release measurements favor a mechanism in which actin-activated P_i release from myosin Va is very rapid, independent of calcium and the tail domain, both heads do not bind actin strongly during steady-state cycling, as assayed by pyrene actin fluorescence. In the absence of calcium, inclusion of ADP favors formation of a long lived myosin Va·ADP state that releases ADP slowly, even after mixing with actin. Our results suggest that calcium activates myosin Va by allowing both heads to interact with actin and exchange bound nucleotide and indicate that regulation of actin binding by the tail is a nucleotide-dependent process favored by linked conformational changes of the motor domain.

Class V myosins participate in a diverse array of cellular functions ranging from organelle transport, mRNA localization and transport, and apoptotic signaling pathways (1, 2). Vertebrate myosin Va, one of three myosins V expressed in vertebrates, is the best characterized of the Class V myosins. Individual double-headed vertebrate myosin Va molecules are processive and take multiple steps along an actin filament before dissociating (3), although not all Class V myosins exhibit processive movement (4). Calcium enhances the steady-state actin-activated ATPase activity but diminishes the *in vitro* motility of full-length myosin Va (5). This regulation is partially due to calcium binding the calmodulin light chains (6–9). A recombinant myosin Va dimer missing the tail is fully activated in the absence of calcium, whereas full-length myosin is not, indicating that additional levels of calcium-dependent regulation are mediated by the C-terminal cargo-binding "tail" domain. Cameron *et al.* (6) described a calcium-dependent change in intrinsic fluorescence of full-length myosin Va, interpreted to reflect a conformational change in the heavy chain. This prediction has since been confirmed by electron microscopy and analytical ultracentrifugation studies that identified a large conformational change of full-length myosin Va from a compact conformation in the absence of calcium to an extended conformation in the presence of calcium (7–9). The compact conformation, believed to represent an enzymatic "off" state, appears to arise from an interaction of the tail with the N-terminal head or light chain-binding "neck" (10, 11). Despite increasing evidence that the tail domain regulates myosin Va motor function, it remains unclear which ATPase cycle transitions are affected in the compact conformation and how calcium activates motor function.

Kinetic parameters of key ATPase cycle events have been measured for individual full-length, tissue-purified myosin Va using single-molecule methods (3, 12, 13). However, these experiments immobilized myosin Va to a surface or a bead by adsorption through the tail and therefore could not explicitly account for tail regulation. Consequently, little is known about how the tail domain regulates the kinetics of myosin Va.

In this study, we have measured actin and nucleotide binding to tissue-purified chick brain myosin Va and have tested the effect of calcium on these parameters. Our results favor a mechanism in which the tail domain of myosin Va interacts with and weakens actin binding to one of the two heads in the absence of calcium and indicate that this interaction is favored by bound ADP. The data suggest that a long lived myosin·ADP state in the absence of actin contributes to the low ATPase activity in the folded "off" state.

MATERIALS AND METHODS

Reagents—All chemicals and reagents were the highest purity commercially available. ATP was purchased from Roche

* This work was supported by American Heart Association Grants 0235203N and 0655849T, and National Science Foundation Grants MCB-0216834 and MCB-0546353 (to E. M. D. L. C.), and National Institutes of Health Grants DK 25387 and GM073823 (to M. S. M.). The costs of publication of this article were defrayed in part by the payment of page charges. This article must therefore be hereby marked "*advertisement*" in accordance with 18 U.S.C. Section 1734 solely to indicate this fact.

[S] The on-line version of this article (available at http://www.jbc.org) contains supplemental Figs. S1–S3.

[1] Supported by National Institutes of Health Predoctoral Fellowship 1F31AR051614-01.

[2] To whom correspondence should be addressed: Yale University, Dept. of Molecular Biophysics and Biochemistry, P.O. Box 208114 New Haven, CT 06520-8114. Tel.: 203-432-5424; Fax: 203-432-1296; E-mail: enrique.delacruz@yale.edu.

Supplemental Material can be found at: http://www.jbc.org/cgi/content/full/M603898200/DC1

Applied Science, and ADP was purchased from Sigma. Mant[3]-labeled nucleotides were prepared as described (14). Nucleotide concentrations were determined by absorbance (15). A molar equivalent of $MgCl_2$ was added to nucleotides immediately before use.

Protein Expression and Purification—Full-length chick brain myosin Va with bound essential light chains and calmodulin was purified from brains of newly hatched chicks (16). Recombinant double-headed chicken myosin Va missing the C-terminal globular tail (tailless myosin V-HMM) was truncated to include 20 native heptad repeats of predicted coiled-coil, followed by a GCN4 leucine zipper to ensure dimerization and a FLAG tag (17). Tailless myosin V-HMM with bound essential light chain and calmodulin was purified from *Sf*9 cells by FLAG affinity chromatography. Purity was >98% for all preparations.

Actin was purified from rabbit skeletal muscle, labeled with pyrene, and gel-filtered over Sephacryl S-300HR (18). Ca^{2+}-actin monomers were converted to Mg^{2+}-actin monomers with 0.2 mM EGTA and 50 μM $MgCl_2$ (excess over [actin]) immediately prior to polymerization by dialysis against KMg50 buffer (50 mM KCl, 2 mM $MgCl_2$, 0.1 mM EGTA, 2 mM dithiothreitol, and 10 mM imidazole, pH 7.0). Phalloidin (1.1 mol eq) was used to stabilize actin filaments.

Equilibrium Titrations—Myosin Va binding to actin filaments was measured from the [myosin] dependence of pyrene actin fluorescence quenching. Native chick brain myosin Va (with or without 1 mM ADP) containing 3 μM exogenous calmodulin was equilibrated with 60 or 100 nM pyrene actin filaments at 25 ± 1 °C for 40–60 min. Apyrase (0.5 units ml^{-1}) was included to achieve rigor (no nucleotide) conditions where indicated. In samples containing calcium, the free [Ca^{2+}] was calculated using the program WinMaxC[32] (Chris Patton, Stanford University) (available on the World Wide Web at www.stanford.edu/~cpatton).

Steady-state fluorescence intensities were measured at 25 ± 1 °C using a thermostatted Photon Technologies Intl. (New Brunswick, NJ) Alphascan fluorescence spectrometer. Binding stoichiometries were obtained by fitting the fluorescence intensities at 405 nm (λ_{ex} = 365 nm) to Equation 1,

$$F(r) = F_o + (F_\infty - F_o) \times \left(\frac{\left(r + \frac{K_d}{A_{tot}} + n\right) - \sqrt{\left(r + \frac{K_d}{A_{tot}} + n\right)^2 - 4 \cdot r \cdot n}}{2 \cdot n} \right) \quad \text{(Eq. 1)}$$

where $F(r)$ represents the fluorescence intensity (F) as a function of the [myosin heads]/[actin] ratio (r), F_o is the fluorescence in the absence of myosin, F_∞ is the fluorescence intensity at infinitely high r (*i.e.* saturating [myosin heads]/[actin]), K_d is the apparent dissociation equilibrium constant of actomyosin, A_{tot} is the total actin concentration, and n is the stoichiometry of myosin Va head binding to actin subunits in a filament (15). The stoichiometry (n), initial (F_o) and final (F_∞) fluorescence were allowed to float when fitting. Values of K_d were constrained to the values calculated from the ratio of the experimentally determined association and dissociation rate constants, except where indicated.

Kinetic Measurements and Analysis—All kinetic experiments were performed at 25 ± 0.1 °C in KMg50 buffer with an Applied Photophysics (Surrey, UK) SX.18MV-R stopped flow apparatus. Concentrations stated are final after mixing. Pyrene (λ_{ex} = 365 nm) and mant nucleotide fluorescence (λ_{ex} = 297 nm) were monitored at 90° from the incident light source through a 400-nm long pass glass filter. Long time courses were corrected for contributions from photobleaching. Most time courses shown are of individual, unaveraged, 1000-point transients collected with the instrument in "oversampling" mode, where the intrinsic time constant for data acquisition is ~30 μs. Typically, multiple (two or three) time courses were averaged before analysis.

Time courses of fluorescence change were fitted to a sum of exponentials using software provided with the instrument. Fitting was limited to data beyond 3 ms to account for the instrument dead time and to exclude data acquired during the continuous flow phase of mixing. Uncertainties are reported as S.E. of the best fits.

Time courses of myosin Va and myosin Va·ADP binding to pyrene actin filaments were measured under pseudo-first order conditions with [actin] ≫ [myosin heads] (15). Myosin Va dissociation from pyrene actin filaments was measured by competition with a large molar excess of unlabeled actin (15).

Time courses of nucleotide (ATP, ADP, mant-ATP, or mant-ADP) binding were acquired under pseudo-first order conditions with [nucleotide] ≫ [myosin or actomyosin]. Actomyosin samples were prepared at a binding density of 0.1–0.2 [myosin heads]/[actin]. ADP binding to actomyosin was measured by kinetic competition with ATP (15, 19). The [ADP] dependence of the observed fast phase rate constant was fitted to Equation 2,

$$k_{fast} = \left(\frac{K'_{1T}k'_{+2T}[ATP] + K'_{1D}k'_{+2D}[ADP]}{1 + K'_{1T}[ATP] + K'_{1D}[ADP]} \right) \quad \text{(Eq. 2)}$$

where K'_{1T} and K'_{1D} are the equilibrium constants for actomyosin·ATP and actomyosin·ADP collision complex formation, respectively, k'_{+2T} is the isomerization rate constant defining the strong (low pyrene fluorescence) to weak (high pyrene fluorescence) actin binding transition, and k'_{+2D} is the isomerization rate constant defining the weak to strong ADP binding transition, as defined by the following two-step nucleotide (N) binding mechanism.

$$AM + N \underset{}{\overset{K'_{1N}}{\rightleftharpoons}} AM(N) \underset{k'_{-2N}}{\overset{k'_{+2N}}{\rightleftharpoons}} AM \cdot N$$

SCHEME 1

Measurement of Oxygen Isotopic Exchange during ATP Hydrolysis—Hydrolysis of ATP was performed in KMg50 buffer containing 50–55% [^{18}O]water supplemented with 2 mM MgATP, 2–4 mM phosphoenolpyruvate (PEP), and 100 units/ml pyruvate kinase to regenerate ATP and prevent accu-

[3] The abbreviations used are: mant, 2(3)-*O*-*N*-methylanthraniloyl; mantATP, 2(3)-*O*-*N*-methylanthraniloyl-ATP; mantADP, 2(3)-*O*-*N*-methylanthraniloyl-ADP.

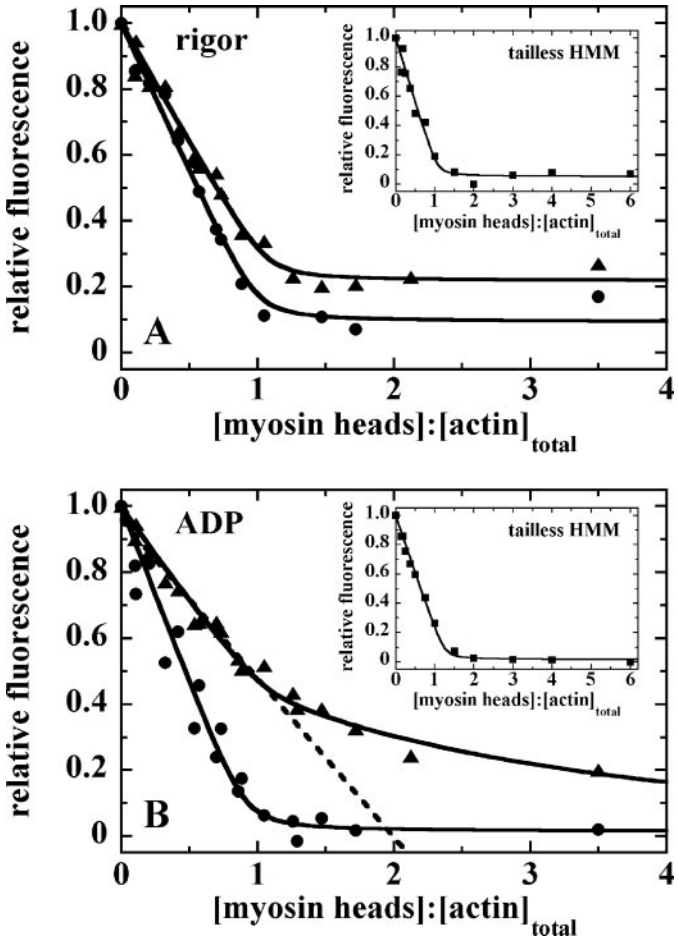

FIGURE 1. **Equilibrium titration of myosin Va with pyrene actin.** *A*, [myosin V] dependence of the pyrene actin fluorescence intensity in the absence of nucleotide. Shown is myosin Va in the absence (▲) and presence (●) of calcium. The *solid lines* represent the best fits to Equation 1. Stoichiometries (*n*) are summarized in Table 1. *Inset*, equilibrium titration of myosin V-HMM with pyrene actin in the absence of calcium. *B*, [myosin V·ADP] dependence of the pyrene actin fluorescence intensity. The *solid line* for myosin Va·ADP (in the absence of calcium) represents the fit for two populations that bind actin with different affinities. The *dotted line* represents the extrapolation of the initial slope of the best fit. *Inset*, equilibrium titration of myosin V-HMM·ADP with pyrene actin in the absence of calcium. The fluorescence intensities were normalized relative to the maximum fluorescence quenching of myosin V-HMM in the absence of nucleotide. Conditions were as follows: 60 or 100 nM pyrene actin, 3 μM excess calmodulin, 0.5 units/ml apyrase (rigor) or 1 mM MgADP (ADP), and varying concentrations of myosin Va or myosin V-HMM to achieve the appropriate myosin heads/actin ratios.

mulation of ADP (20). The reactions were quenched with acid, and the P_i was isolated and analyzed for ^{18}O content (21).

RESULTS

Equilibrium Titration of Pyrene Actin and Myosin Va—Myosin Va binding quenches the fluorescence of pyrene actin filaments in the presence and absence of calcium (22), allowing for "strong" actin binding, using the definition of Geeves (23), to be monitored from changes in fluorescence. At equilibrium, both heads of tissue-purified myosin Va (no bound nucleotide) bind actin strongly (Fig. 1*A*) with K_d values of ≤1 nM. With bound ADP (≥1 mM MgADP), both heads bind actin strongly as indicated by the levels of pyrene fluorescence quenching (Fig. 1*B*). However, the titrations are best described by two approximately equal phases with different apparent actin affinities: one that binds strongly ($K_d^{app} < 1$ nM) and a second that binds more weakly ($K_d^{app} > 100$ nM).

The two apparent affinities observed in the equilibrium binding isotherms could arise if one head of myosin Va bound actin strongly ($K_d < 1$ nM; quenched pyrene) and the other weakly ($K_d \gg 1$ nM; did not quench pyrene), and the weakly bound or detached head competed with strong binding of free, incoming myosin Va molecules. The inflection point extrapolated from the initial slope is ~2 (*i.e.* behaves as a 1:1 myosin Va-actin subunit complex until half-saturation is reached; Fig. 1*B*), as expected for such a binding mechanism. If each myosin Va head bound to adjacent sites on a filament, it is expected that the number of available adjacent subunits would decrease as the myosin binding density increased (*i.e.* a manifestation of the "parking problem") (24). This behavior would also yield a titration profile that deviates significantly from a hyperbola (Fig. 1*B*). However, kinetic data obtained with actin in excess over myosin (presented below), which eliminates the parking problem, is consistent with the interpretation that one head of myosin Va·ADP is weakly bound to or detached from actin in the absence of calcium. A mechanism in which a mixed population of myosin Va molecules (*i.e.* one that binds with $K_d < 1$ nM and another that binds both heads with $K_d > 100$ nM) can be eliminated, since this would not yield a biphasic titration. We therefore favor a mechanism in which the two heads of myosin Va·ADP bind actin with different affinities in the absence of calcium; one is strongly bound (quenched pyrene), and the other is weakly bound or detached (unquenched pyrene).

The ADP-dependent head asymmetry occurs only in the absence of calcium. When calcium is present, both heads of myosin Va bind actin strongly in rigor and in the presence of ADP (Fig. 1*A*; $1/K_A^{app} \leq 1$ nM in rigor and $1/K_{AD}^{app} < 1$ nM with ADP).

Both heads of recombinant myosin V-HMM missing the C-terminal cargo-binding tail bind actin strongly (Fig. 1, *A* and *B*, *insets*) in the presence and absence of ADP and in the absence of calcium ($1/K_A^{app} \leq 1$ nM in rigor and $1/K_{AD}^{app} < 1$ nM with ADP), indicating that the effect of ADP on two-headed actin binding is unique to full-length myosin Va and is presumably mediated through the tail domain.

Kinetics of Myosin Va Binding to Actin Filaments—Time courses of fluorescence quenching after mixing pyrene actin filaments with myosin Va or myosin Va·ADP follow double exponentials both in the presence and absence of calcium (Fig. 2, *A* and *B*) with fast phase observed rate constants that depend linearly on [actin] (Fig. 2, *C* and *D*), as described for single-headed myosin V-S1 (14) and tailless recombinant myosin V-HMM (25). The slow phases comprised ~50% of the total amplitudes in the absence of calcium and were smaller in the presence of calcium (Fig. 2, *A* and *B*). In this report, we focus our kinetic analysis only on the fast phases, because the data cannot distinguish between a sequential reaction mechanism (14) or a mixed population of myosin (heads or conformational states). The $[Ca^{2+}]$ dependence of the relative amplitudes favors a reversible calcium-dependent equilibrium as reported for scallop myosin HMM (24, 26).

The apparent association rate constants for actin filament binding were obtained from the slopes of the lines generated by plotting the observed pseudo-first order rate constant (k_{obs}) *versus* [actin] (Fig. 2, *C* and *D*). Under rigor conditions, binding (k_{+A}) was ~16 μM^{-1} s^{-1} in the absence of calcium and almost twice as fast when calcium was present (~28 μM^{-1} s^{-1}). Bound ADP slows the association rate constant (k_{+AD}) about 4-fold from ~16 μM^{-1} s^{-1} to ~4 μM^{-1} s^{-1} in the absence of calcium (Table 1 and Scheme 2); ADP has a smaller effect (~2-fold reduction) on the association kinetics when calcium is present (Table 1 and Scheme 2). Tailless myosin V with bound ADP binds actin filaments with an association rate constant of 16–19 μM^{-1} s^{-1} in the absence of calcium (25), suggesting that the tail domain slows actin binding only when ADP is bound.

The total pyrene quenching amplitudes of myosin Va with bound ADP in the absence of calcium averaged 53 ± 9% of the amplitudes in the presence of calcium over the [actin] range examined (0.1–0.8 μM). We interpret this to mean that when calcium is absent, one head binds actin strongly and rapidly upon encounter, but the other remains weakly bound or detached and does not quench fluorescence. In rigor, the total quenching amplitudes in the presence and absence of calcium

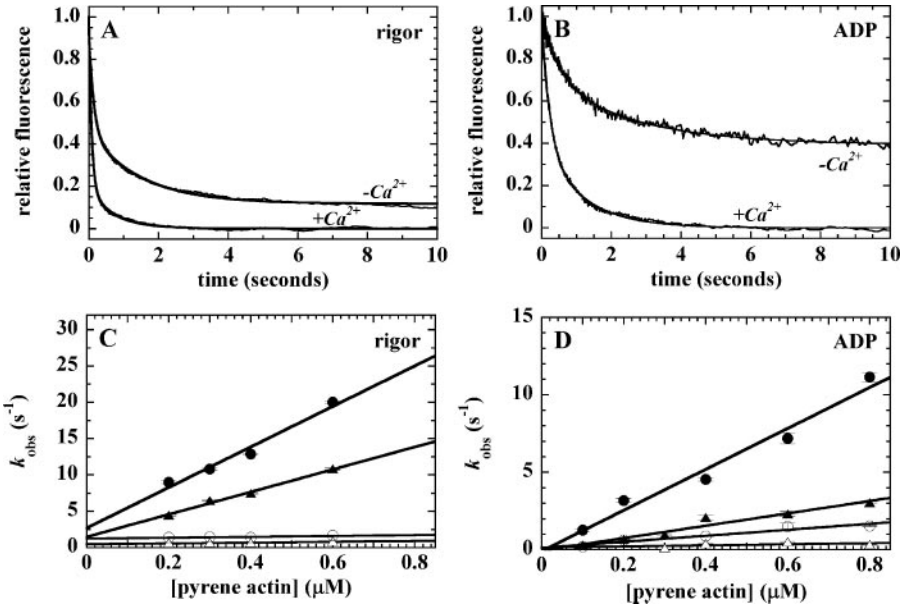

FIGURE 2. **Kinetics of pyrene actin binding to myosin Va.** *A*, time courses of pyrene fluorescence quenching after mixing 40 nM myosin Va heads in rigor with 400 nM pyrene actin, 3.5 μM excess calmodulin, and 1.1 mM EGTA ($-Ca^{2+}$) or 100 μM free Ca^{2+} ($+Ca^{2+}$). The data shown are the averages of two individual transients. The *smooth lines* through the data represent the best fits to double exponentials. Slow phases comprised 25–40% of total amplitude. *B*, time courses of pyrene fluorescence quenching after mixing myosin Va with pyrene actin in the presence of 2 mM MgADP using concentrations defined in *A*. The data shown are the averages of two individual transients. The *smooth lines* through the data represent the best fits to double exponentials. Slow phases comprised ~40% of total amplitude. *C*, [pyrene actin] dependence of the observed rate constants for myosin Va binding to pyrene actin filaments in the absence (▲, fast phase; △, slow phase) or presence (●, fast phase; ○, slow phase) of 100 μM free Ca^{2+}. The *solid lines* are the best fits to linear functions with slopes of 15.5 μM^{-1} s^{-1} for myosin Va in the absence of free Ca^{2+} and 27.9 μM^{-1} s^{-1} (fast phase). *D*, [pyrene actin] dependence of the observed rates for myosin Va·ADP binding to pyrene actin filaments in the absence (▲, fast phase; △, slow phase) or presence (●, fast phase; ○, slow phase) of 100 μM free Ca^{2+}. The *solid lines* are the best fits to linear functions with fast phase slopes of 4.0 μM^{-1} s^{-1} for myosin Va·ADP in the absence of free Ca^{2+} and 13.2 μM^{-1} s^{-1} in the presence of free Ca^{2+}.

TABLE 1

Summary of kinetic and equilibrium constants for calcium-regulated nucleotide and actin binding to native actomyosin Va

	Tissue-purified myosin Va (EGTA)[a]	Tissue-purified myosin Va ($CaCl_2$)[b]	Tailless myosin V-HMM (EGTA)[a]	Tailless myosin V-HMM ($CaCl_2$)[b]
ATP binding				
$K_{1T}k_{+2T}$ (μM^{-1} s^{-1}), mantATP	1.6 ± 0.2	1.3 ± 0.2	ND[c]	ND
$K'_{1T}k'_{+2T}$ (μM^{-1} s^{-1})	1.4 ± 0.2	1.7 ± 0.6	1.2 ± 0.2	1.3 ± 0.6
$1/K'_{1T}$ (μM)	680 ± 89	509 ± 162	1095 ± 165	955 ± 395
k'_{+2T} (s^{-1})	941 ± 65	874 ± 120	1297 ± 113	1277 ± 293
ADP binding				
$K'_{1D}k'_{+2D}$ (μM^{-1} s^{-1})	5.2 ± 0.9	43 ± 7.3	42 ± 9	148 ± 77
$1/K'_{1D}$ (μM)	79 ± 13	21 ± 3	14 ± 3	6 ± 3
k'_{2D} (s^{-1})	408 ± 32	902 ± 61	589 ± 42	890 ± 123
k'_{-2D} (s^{-1}), mantADP·P_i[d]	10.0 ± 1.1	11.9 ± 4.7	ND	ND
$K'_{2D} = k'_{+2D}/k'_{-2D}$	40.8 ± 4.5	75.8 ± 29.9	ND	ND
$1/K'_{1D}K'_{2D}$ (μM)	1.9 ± 0.2	0.3 ± 0.1	ND	ND
Actin binding				
k_{+A} (μM^{-1} s^{-1})	15.5 ± 1.1	27.9 ± 3.3	ND	ND
k_{-A} (s^{-1})	0.36 ± 0.02	0.004 ± <0.001	ND	ND
k_{+AD} (μM^{-1} s^{-1})	4.0 ± 0.5	13.2 ± 1.3	16–19[e]	ND
k_{-AD} (s^{-1})	0.03 ± 0.002, 0.004 ± <0.001	0.008 ± <0.001	ND	ND
n (rigor)[f]	1.1 ± 0.1	1.0 ± 0.1	1.1 ± 0.1	ND
n (2 mM MgADP)[f]	~2[g]	0.9 ± 0.1	1.2 ± 0.1	ND

[a] 10 mM imidazole, pH 7.0, 50 mM KCl, 2 mM $MgCl_2$, 1.1 mM EGTA, 2 mM DTT, 25 °C.
[b] 10 mM imidazole, pH 7.0, 50 mM KCl, 2 mM $MgCl_2$, 0.1 mM EGTA, 0.2 mM $CaCl_2$, 2 mM DTT, 25 °C.
[c] ND, not detected.
[d] Sequential mix monitoring mant fluorescence (λ_{ex} = 297 nm).
[e] Measured in 25 mM HEPES, 50 mM KCl, 2 mM $MgCl_2$, 1 mM EGTA, 1 mM dithiothreitol, pH 7.5, 20 °C (25).
[f] n = stoichiometry of myosin heads per actin subunit.
[g] Determined from extrapolated fit (Fig. 1*B*).

$$\begin{array}{ccccccccccccc}
AM + ATP & \overset{K_{1T}'}{\rightleftharpoons} & AM(ATP) & \overset{K_{2T}'}{\rightleftharpoons} & AM{\cdot}ATP & \overset{K_{H}'}{\rightleftharpoons} & AM{\cdot}ADP{\cdot}P_i & \overset{K_{Pi}'}{\rightleftharpoons} & AM{\cdot}ADP & \overset{K_{2D}'}{\rightleftharpoons} & AM(ADP) & \overset{K_{1D}'}{\rightleftharpoons} & AM + ADP \\
K_A \updownarrow & & \updownarrow & & K_{diss} \updownarrow & & K_{APi} \updownarrow & & K_{AD} \updownarrow & & \updownarrow & & K_A \updownarrow \\
M + ATP & \overset{K_{1T}}{\rightleftharpoons} & M(ATP) & \overset{K_{2T}}{\rightleftharpoons} & M{\cdot}ATP & \overset{K_{H}}{\rightleftharpoons} & M{\cdot}ADP{\cdot}P_i & \overset{K_{Pi}}{\rightleftharpoons} & M{\cdot}ADP & \overset{K_{2D}}{\rightleftharpoons} & M(ADP) & \overset{K_{1D}}{\rightleftharpoons} & M + ADP
\end{array}$$

SCHEME 2

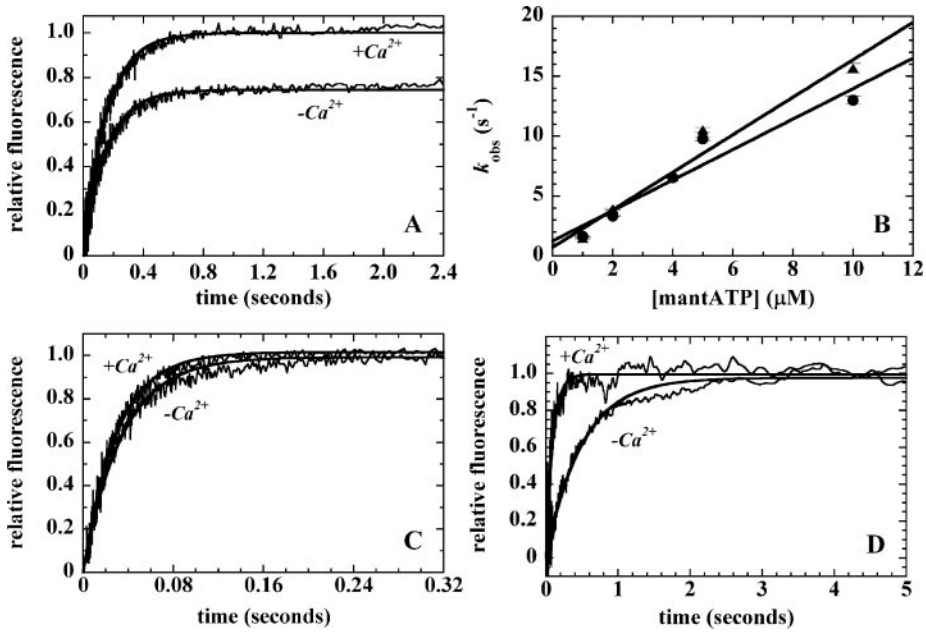

FIGURE 3. **Kinetics of mant-nucleotide binding to myosin Va.** *A*, time course of fluorescence enhancement upon mantATP binding to myosin Va in the absence ($-Ca^{2+}$) and presence of 100 μM free Ca^{2+} ($+Ca^{2+}$). Final concentrations are 100 nM myosin Va heads, 3.1 μM excess calmodulin, and 4 μM mantATP. The traces are of raw, unaveraged individual transients. The *smooth lines* through the data represent the best fits to single exponentials yielding an identical rate of 6.6 ± 0.1 s^{-1} in the absence and presence of calcium. *B*, [mantATP] dependence of the observed rates for myosin Va binding to mantATP in the absence (▲) or presence (●) of 100 μM free Ca^{2+}. The *solid lines* are the best fits to linear functions with slopes of 1.6 μM^{-1} s^{-1} for myosin Va in the absence of free Ca^{2+} (●) and 1.2 μM^{-1} s^{-1} for myosin Va in the presence of 100 μM free Ca^{2+} (○). *C*, time course of fluorescence enhancement upon mantATP binding to tailless myosin V-HMM in the absence ($-Ca^{2+}$) and presence of 100 μM free Ca^{2+} ($+Ca^{2+}$). Final concentrations are 500 nM myosin V heads, 3.1 μM excess calmodulin, and 14 μM mantATP. The traces are an average of three individual transients. The *smooth lines* through the data represent the best fits to single exponentials. *D*, time course of fluorescence enhancement upon mantADP binding to myosin Va in the absence ($-Ca^{2+}$) and presence of 100 μM free Ca^{2+} ($+Ca^{2+}$). Final conditions are 50 nM myosin Va heads, 1.5 μM excess calmodulin, and 2.5 μM mantADP. The *smooth lines* through the data represent the best fits to single exponentials yielding rates of 2.0 ± 0.1 s^{-1} in the absence of calcium and 11.0 ± 0.3 s^{-1} in the presence of calcium.

differ by ~10%, consistent with calcium-regulated actin binding requiring ADP, presumably bound to the myosin motor domain.

The equilibrium titrations (Fig. 1) suggest that only one head of myosin Va·ADP binds actin strongly in the absence of calcium. The observation that the quenching amplitudes in the kinetic time courses (with [actin] ≫ [myosin]) do not change over a range of [actin] is consistent with this mechanism. If two myosin Va populations existed in solution (one that bound actin strongly with both heads and the other weakly with both heads), all myosin Va molecules would bind and quench pyrene actin fluorescence at saturating [actin] (≥0.5 μM), and this is not observed.

Time courses of actomyosin Va dissociation follow single exponentials in the presence and absence of calcium (Table 1 and Scheme 2) (data not shown). Actomyosin Va·ADP dissociation follows double exponentials in the absence of calcium and is well described by a single relaxation in the presence of calcium (Table 1 and Scheme 2) (data not shown). Rapid dissociation is not observed in the presence of calcium, suggesting that calcium shifts the population to a slowly dissociating species and that the actin filament binding affinity is tighter in the presence of calcium, as inferred from previous studies (22).

MantATP and MantADP Binding to Myosin Va—Mant-nucleotide binding to myosin Va in the absence of actin was measured from the fluorescence enhancement that occurs with binding (27). Time courses of mantATP binding (Fig. 3*A*) are well fitted by single exponentials with observed rate constants that depend linearly on [mantATP] (Fig. 3*B*). Calcium does not affect the mantATP association rate constant (~1 μM^{-1} s^{-1} in the presence and absence of calcium) (Table 1 and Scheme 2). However, the amplitudes of the fluorescence enhancement are ~30 ± 6% lower in the absence of calcium over the range examined (Fig. 3*A*) (data not shown). We can exclude the possibility that bound, contaminating nucleotide (*i.e.* ADP) lowers the concentrations of heads capable of binding mantATP, thus lowering the amplitude, because this would yield a biphasic time course (*i.e.* rapid binding to vacant sites and slow binding to occupied sites upon dissociation of bound nucleotides), which was not observed (Fig. 3*A*). In addition, treatment of myosin with apyrase had no effect (data not shown). However, if bound nucleotide were trapped and did not readily dissociate, time courses of mantATP and mantADP binding would follow single exponentials with lower amplitudes as observed. The fact that the amplitudes of mantADP fluorescence change are similar in the absence and presence of calcium (Fig. 3*D*) is consistent with the interpretation that trapped, slowly exchanging or nonexchanging nucleotide does not account for the observed amplitude difference.

The amplitudes of mantATP binding to tailless myosin V-HMM are identical in the presence and absence of calcium (Fig. 3*C*), suggesting that the calcium-dependent amplitudes

observed with full-length myosin Va arise from calcium-dependent, tail-specific interactions with the motor domain(s).

MgATP Binding to Actomyosin Va—ATP binding to actomyosin Va was monitored from changes in pyrene actin fluorescence enhancement that arise with population of the weak binding actomyosin·ATP states. To ensure that all reactions end with complete dissociation of actomyosin from pyrene actin, excess unlabeled F-actin was included in the ATP syringe. Time courses of pyrene fluorescence enhancement (Fig. 4*A*) after mixing pyrene actomyosin Va with ATP (in the absence or presence of free calcium) follow double exponentials with fast observed rate constants (k_{fast}) that depend hyperbolically on ATP concentration (Fig. 4*B*), consistent with a two-step mechanism for ATP binding to actomyosin Va (Scheme 1). There was also a slow phase that displays little [ATP] dependence in the absence and presence of calcium with rates (k_{slow}) varying between ~1 and 2 s^{-1}, ~500–1000-fold slower than the maximum rate of ATP-induced population of the weak actin binding state of myosin Va (k'_{+2T} = 941 s^{-1} in the absence of calcium and 874 s^{-1} in the presence of calcium) (Fig. 3*B*, Table 1, and Scheme 2) and ~10-fold slower than the rate of ADP release (12–15 s^{-1}) from actomyosin V-S1 (20, 27). We interpret this slow phase to represent (two-headed) myosin Va dissociation from actin filaments (28), which was confirmed by light scattering (data not shown).

Calcium does not significantly affect the kinetics of ATP binding to actomyosin Va. In the absence of free calcium, the second order ATP association rate constant ($K'_{1T}k'_{+2T}$) is 1.4 μM^{-1} s^{-1} (Table 1 and Scheme 2). In the presence of free calcium, it is 1.7 μM^{-1} s^{-1} (Table 1 and Scheme 2).

The ATP binding rate constants reported here in the presence of calcium are in agreement with values obtained for single-headed myosin Va in transient kinetic solution studies (19, 27) and double-headed myosin V in single molecule measurements (12, 29), indicating that the intramolecular strain generated from the second head binding to actin does not affect ATP binding, presumably to the trailing head.

MgADP Binding to Actomyosin Va—ADP binding to pyrene actomyosin Va was measured by kinetic competition with ATP (15, 19). Time courses of pyrene fluorescence enhancement after mixing pyrene actomyosin Va with a solution of ADP and ATP are biphasic and can be well fitted to double exponentials (Fig. 5*A*). The [ADP] dependence of the fast phase can be used to extract the ADP association rate constant and binding mechanism (Equation 2) (15). The hyperbolic [ADP] dependence of the fast phase observed rate constant (Fig. 5*B*) indicates that ADP binding to actomyosin Va in the absence and presence of free calcium is (at least) a two-step process (Scheme 1), similar to recombinant single-headed myosin V-S1 (19).

Calcium accelerates ADP binding to actomyosin Va almost 10-fold compared with calcium-free conditions. In the absence of calcium, the second order rate constant for ADP binding to actomyosin Va ($K'_{1DT}k'_{+2D}$) is 5.2 μM^{-1} s^{-1}. In the presence of free calcium, the rate constant for ADP binding to actomyosin Va ($K'_{1D}k'_{+2D}$) is 43 μM^{-1} s^{-1} (Table 1 and Scheme 2). The more rapid association rate constant arises from a tighter equilibrium constant for collision complex formation (K'_{1D}) and a ~2-fold faster isomerization rate constant (k'_{+2D}).

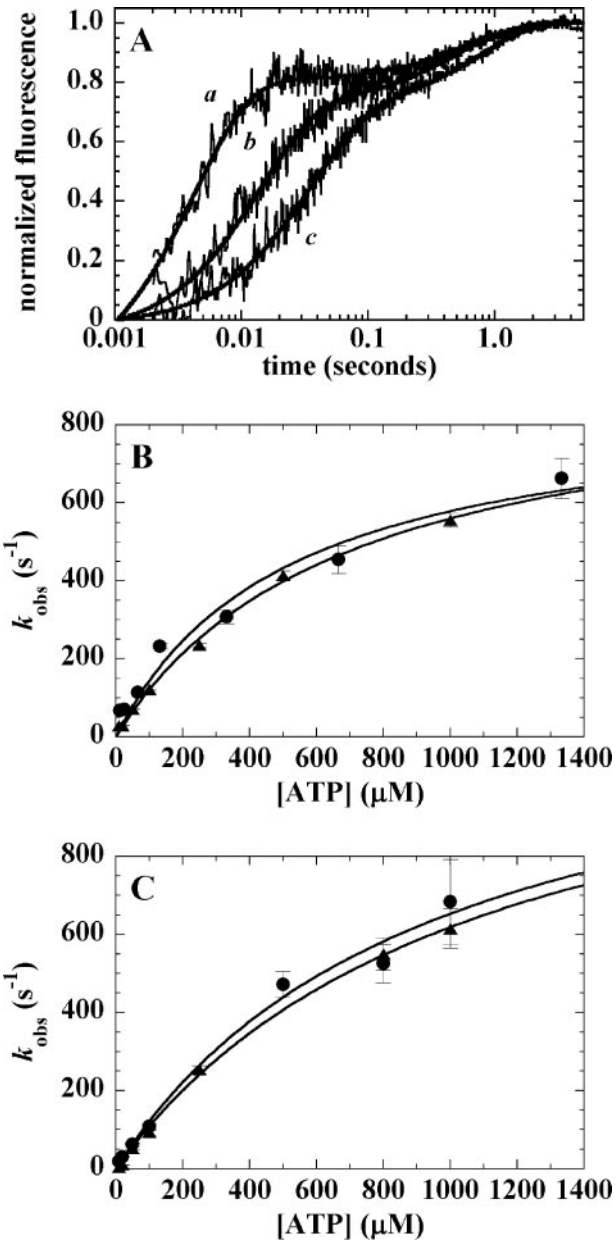

FIGURE 4. **Kinetics of ATP binding to actomyosin Va.** *A*, time courses of pyrene fluorescence enhancement after mixing 15 nM myosin Va heads, 3.3 μM excess calmodulin, and 100 nM pyrene actin with 250 (*a*), 50 (*b*), and 20 μM (*c*) MgATP in the absence of free Ca^{2+} (≥1 mM EGTA). Unlabeled actin (1 μM) was included with ATP to prevent completely dissociated myosin Va molecules from rebinding to pyrene actin. The data shown are of single, unaveraged transients. The *smooth lines* through the data represent the best fits to double exponentials. *B* and *C*, [ATP] dependence of the observed rate constant (k_{obs}) of MgATP binding to actomyosin Va (*B*) and tailless actomyosin V-HMM (*C*) in the absence (▲) or presence of 100 μM free Ca^{2+} (●). The *solid lines* through the data are the best fits to Equation 2 (where [ADP] = 0; see Table 1 for values). The slow phase varied between ~1 and 2 s^{-1} and did not depend strongly on [ATP].

In previous studies with single-headed myosin V (19) and myosin VI (15), observed slow phases in the presence of ADP were used to extract the ADP dissociation rate constant (k'_{-2D}) and the relative ADP and ATP binding affinities. However, we did not attempt to analyze the slow phases observed in this study because of the pronounced slow phase present with ATP alone (Fig. 1), which was absent from single-headed myosin V

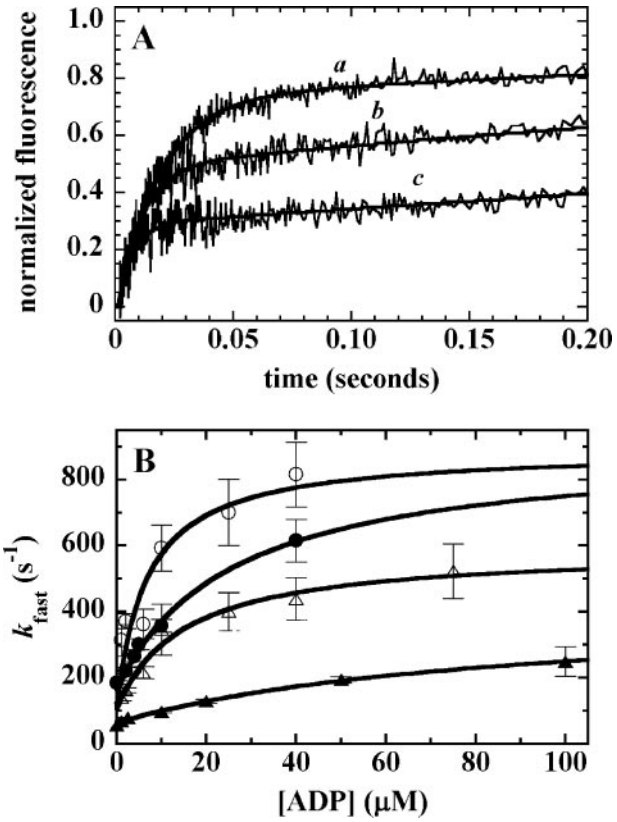

FIGURE 5. **Kinetics of ADP binding to actomyosin Va.** *A*, time courses of pyrene fluorescence enhancement after mixing 15 nM myosin Va heads, 3.3 μM calmodulin, and 100 nM pyrene actin with 50 μM MgATP containing 0 (*a*), 10 (*b*), and 50 μM (*c*) MgADP in the absence of free Ca^{2+}. The data shown are of single, unaveraged transients. The *smooth lines* through the data represent the best fits to double exponentials. *B*, [ADP] dependence of the fast phase rate constant after mixing 100 nM pyrene actin and 20 nM myosin Va heads with 50 μM MgATP and varying concentrations of MgADP in the absence of free Ca^{2+} (▲) or with 120 μM MgATP and varying concentrations of MgADP in the presence of 100 μM free Ca^{2+} (●). Similar experiments were performed, mixing 20 nM tailless myosin V-HMM and 100 nM pyrene actin with 100 μM MgATP and varying concentrations of MgADP in the absence (△) and presence of 100 μM free Ca^{2+} (○). The *solid lines* through the data are the best fit to Equation 2 (15, 19).

and interpreted to reflect double-headed dissociation from actin (discussed above).

^{18}O Exchange Experiments with Myosin Va—Oxygen isotopic exchange can provide an estimate of the partitioning of the *E*·ADP·P_i complex between release of P_i and reversal of hydrolysis to reform *E*·ATP (where *E* represents myosin or actomyosin) and has been a useful probe of the mechanism of skeletal muscle myosin II (30–33). Reversible hydrolysis of *E*·ATP to *E*·ADP·P_i before release of P_i can incorporate multiple oxygen atoms from water into P_i. The partition coefficient (*Pc*) reflects the fraction of *E*·ADP·P_i that reverts to *E*·ATP rather than releasing P_i to generate *E*·ADP and is related to the *overall* P_i release and ATP resynthesis rate constants (see Scheme 2) according to the following, $Pc = k_{-H,\,overall}/(k_{-H,\,overall} + k_{P_i,\,overall})$. *Pc* values for a random process can be calculated from the extent of incorporation of water-derived oxygens (21).

Analysis of the extent of isotopic exchange when unenriched ATP is hydrolyzed by single-headed myosin V-S1 in [^{18}O]water indicates that Pc is 0.17 (see supplemental material for detailed analysis) at a near saturating actin concentration of 18 μM. This corresponds to a rate of P_i release rate constant ($k_{P_i,\,overall}$) that is ~5 times faster than the rate of ATP resynthesis ($k_{-H,\,overall}$), consistent with rapid P_i release (~100–300 s^{-1}) upon the initial encounter with actin filaments (25, 27, 29, 34, 35) and the estimated rate constant of ATP resynthesis when detached from actin (34). Similar low *Pc* values of 0.16 and 0.23 were observed with double-headed tissue-purified myosin Va at 12 μM actin in the presence and absence of calcium, respectively, indicating that actin-activated P_i release from myosin Va is 3–5 times faster than ATP resynthesis and is not significantly affected by calcium.

Actin-activated Product Release of Myosin Va—To determine if calcium affects actin-activated product release from myosin Va, we performed a sequential mixing experiment where myosin Va with or without calcium was first mixed with excess mantATP, allowed to age for 2 s, and then mixed with actin filaments and unlabeled ATP. The best fits of the time courses (Fig. 6*A*) to single exponentials were reasonable, given the signal to noise ratio. However, the data are best described by two phases, as indicated by the residuals and χ^2 values of the fits, as reported for myosin V-S1 and tailless myosin V-HMM (25).

The fast phase is thought to represent actin-activated P_i release (25). The fast phase had an observed rate constant of ~40–80 s^{-1} at 19 μM actin (Fig. 6), comparable with values reported for single-headed (25, 27, 29) and double-headed (25) myosin V at the same [actin], and is consistent with the low levels of ^{18}O exchange at high [actin].

The observed rate constants of the slow phases were comparable under both conditions (~11 s) and are likely to represent mantADP release (14, 20, 27), which is limited by a conformational change that precedes and limits rapid ADP dissociation (Scheme 1) (19).

We also measured mantADP release from an equilibrated myosin Va·mantADP mixture. In the presence of calcium (*i.e.* extended conformation), myosin Va behaves very similarly to unregulated myosin V-S1 in that actin binding accelerates mantADP release. More specifically, mantADP release is biphasic in the absence of actin (Fig. 6*B*; fast phase occurring at 5.8 ± 0.3 s^{-1}, comprising ~50% of total amplitude, and slow phase at ~0.5–1 s^{-1}), interpreted to represent two myosin V·mantADP states (one that releases mantADP slowly and one that releases quickly), and actin shifts the equilibrium to favor formation of the rapidly exchanging species (14) (fast phase at 8.8 ± 0.1 s^{-1}, comprising ~85% of total amplitude, and slow phase at ~0.5–1 s^{-1}).

In contrast, *overall* mantADP release in the absence of calcium (*i.e.* folded conformation) is slow and weakly accelerated by actin (Fig. 6*C*). MantADP release from myosin Va is biphasic in the absence of actin and calcium (Fig. 6*C*; fast phase at 1.4 ± 0.1 s^{-1}, comprising ~50% of total amplitude, and slow phase at ~0.5 s^{-1}). Actin binding shifts the equilibrium to favor the rapidly dissociating species (fast phase of 1.7 ± 0.1 s^{-1}, comprising ~90% of total amplitude), as in the presence of calcium. The slower overall mantADP release rate constant arises because fast dissociation is slower from the folded conformation than the extended conformation, consistent with the head-tail interaction stabilizing a long lived myosin V·ADP state that exchanges bound nucleotide slowly, even in the presence of actin.

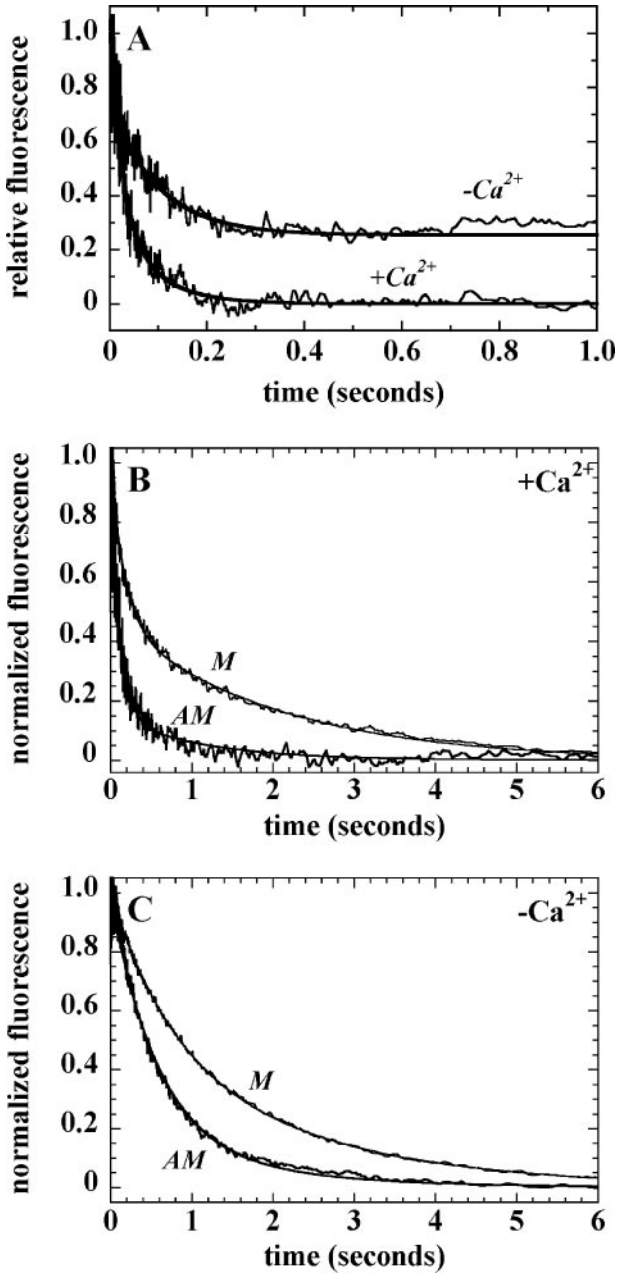

FIGURE 6. **Calcium-regulated actin-activated product release from myosin Va.** *A*, kinetics of actin-activated product dissociation from myosin Va·mantADP·P_i after rapidly mixing with saturating F-actin and unlabeled ATP. Final concentrations are 125 nM myosin Va heads, 31 μM mantADP·P_i, 19 μM F-actin, 1 mM MgATP, and 1 mM EGTA ($-Ca^{2+}$) or 100 μM free Ca^{2+} ($+Ca^{2+}$). The data shown are of single, unaveraged transients. The *smooth lines* are the best fits to double exponentials. The total amplitude of mant fluorescence decay in the absence of calcium reached ~70% of the amplitude in the presence of calcium. *B* and *C*, kinetics of mantADP release from myosin Va·mantADP after mixing with unlabeled ATP in the presence (*AM*) or absence (*M*) of actin and in the presence (*B*) or absence (*C*) of calcium. Final concentrations are 70 nM myosin Va heads, 14 μM mantADP, 10 μM F-actin, 1 mM MgATP, and 100 μM free Ca^{2+} (*B*) or 1 mM EGTA (*C*). The data shown are the averages of two individual transients. The *smooth lines* are the best fits to double exponentials.

DISCUSSION

The Tail Domain of Myosin Va Weakens Actin Binding Affinity of One Head in a Nucleotide-dependent Manner—In the absence of calcium, conditions that favor the folded conformation of myosin Va (7–11), bound ADP weakens the affinity of one head for actin filaments at equilibrium (Fig. 1) and upon initial encounter (Fig. 2). Both heads bind strongly (Fig. 1) and rapidly (Fig. 2) under rigor conditions. The effect of ADP in weakening myosin Va actin affinity is not observed with tailless myosin V-HMM, indicating that this behavior arises from tail-specific allosteric interactions, presumably with one of the two motor domains, since the tail does not interact with actin (36). The fact that the inhibition is observed more prominently when ADP is bound strongly suggests that nucleotide-linked conformational changes of the motor domain (14, 19, 37) favor the motor domain-tail interactions that regulate actin binding.

Inclusion of calcium favors the unfolded conformation of myosin Va (7–9) and promotes strong actin binding of both heads, even in the presence of excess ADP. We interpret this to mean that calcium binding to myosin Va, presumably to the associated calmodulin light chains (but sites on myosin are also possible), weakens the motor domain-tail interaction and allows both heads to readily bind actin strongly at equilibrium (Fig. 1) and upon the initial encounter (Fig. 2), similar to tailless myosin V-HMM. It is anticipated that cargo binding to the tail domain would have similar effects.

The effect of calcium on myosin Va shares striking similarities with calcium regulation of scallop myosin II. As with myosin Va, calcium activates scallop myosin II-HMM ATPase activity and favors the transition from a folded "off" conformation to an extended "on" state (47). In addition, as we report for myosin Va in this study, bound ADP favors formation of the "off" state of scallop HMM, characterized by lower actin-activated ATPase and weak actin binding activities (24, 26). We favor a mechanism in which calcium and ADP affect the reversible folded ("off")-extended ("on") equilibrium of myosin Va in an allosteric manner, similar to scallop HMM (24); calcium promotes the extended conformation, and bound ADP stabilizes the compact, folded conformation. We hypothesize that cargo binding to myosin Va in cells will weaken the head domain-tail interaction, similar to calcium.

Two studies of myosin Va that were published while this manuscript was under review (10, 11) are consistent with the observations and interpretations reported here. Liu *et al.* (11) observe single-headed binding of myosin Va in the presence of ADP and P_i at low myosin/actin ratios, consistent with the tail domain preventing strong two-headed binding to actin, as observed here in the presence of ADP (Figs. 1 and 2). Thirumurugan *et al.* (10) demonstrate that a small fraction of the myosin Va population binds actin in the presence of ATP and in the absence of calcium. This observation can be accounted for if myosin Va bound actin with only one head, as reported here, since the duty ratio of single-headed attachments in the presence of ATP will be small at low actin concentrations (20).

It is surprising that myosin Va and tailless myosin V-HMM can fully saturate actin and display no manifestation of the parking problem, particularly since the long regulatory domains would allow a myosin V dimer to bind actin with a large, variable number of sites between the two heads. Such an observation raises the possibility that myosin V binding induces changes in conformation and/or dynamics (38) that promote binding to actin, perhaps to lateral or longitudinal adjacent subunits.

Bound ADP Strengthens the Head-Tail Domain Interaction—The amplitude of mantATP fluorescence change upon binding myosin Va, but not tailless myosin V-HMM (Fig. 3), is smaller under conditions that favor the folded conformation (*i.e.* amplitudes are ~30% smaller in the absence of calcium). This suggests that the tail interacts with at least one motor domain and inhibits mantATP binding to nucleotide-free actomyosin and/or changes the local environment of the bound nucleotide (mantADP or mantADP·P_i), so that the total fluorescence change is smaller. One possibility is that one or both heads are trapped in a mantADP-like state, which has a lower fluorescence (25). The observation that mantADP binding amplitudes are comparable with and without calcium (Fig. 3*D*) suggests that both heads can bind nucleotide and that the head-tail interaction, although it occurs in the presence of ADP, does not quench the fluorescence of myosin·mantADP.

The kinetics of actin binding are consistent with the head-tail interaction being nucleotide-linked. In the absence of bound nucleotide, both heads of the folded conformation of myosin Va bind actin rapidly. With bound ADP, only one head of folded myosin Va binds and quenches pyrene actin fluorescence upon encounter and at equilibrium (Figs. 1 and 2), consistent with bound ADP favoring interaction of the tail with the motor domain(s).

The kinetics of actin-activated product release are also consistent with a nucleotide-dependent head-tail interaction and suggest that the strength of this interaction (*i.e.* the folded-unfolded equilibrium constant) depends on the chemical state of the bound nucleotide and conformational state of the motor. Sequential mixing experiments in which mantATP is mixed with myosin Va followed by mixing with actin allow for rapid release of hydrolysis products (P_i at $>50\ s^{-1}$ and mantADP at $\sim 11\ s^{-1}$) independent of calcium. MantADP release from an equilibrated myosin Va·mantADP mixture is accelerated by actin in the presence of calcium (*i.e.* extended conformation), similar to single-headed myosin V. However, mantADP release is slow and weakly accelerated by actin (Fig. 6*B*) in the absence of calcium (*i.e.* folded conformation), indicating that head-tail interactions stabilize a long lived myosin·ADP state that is distinct from nucleotide-free myosin Va and myosin Va·ADP·P_i. Therefore, the long lived ADP state is populated with the addition of ADP to nucleotide-free myosin but not through hydrolysis of ATP and may represent the α-state described by Hannemann *et al.* (14). The maximum actin-activated steady-state ATPase rate in the absence of calcium is 1–2 s^{-1} (5) (data not shown) and may be limited by actin-activated ADP release from the long lived actomyosin Va·ADP state. This implies that during steady-state cycling and processive walking, myosin Va dissociates from actin with at least one head in an ADP-bound state, and this state is stabilized through interactions with the tail domain.

Calcium Accelerates ADP but Not ATP Binding to Actomyosin Va Independent of the Tail Domain—ATP and ADP bind actomyosin Va following a two-step reaction mechanism as with single-headed myosin V (19). Calcium does not affect ATP binding ($K'_{1T}K'_{+1T}$) but accelerates the ADP association rate constant ($K'_{1D}k'_{+2D}$) ~8-fold from ~5 to ~40 $\mu M^{-1}\ s^{-1}$ (Table 1 and Scheme 2). This effect of calcium on the ADP binding kinetics does not arise from interactions of the tail with the motor domain, since it is also observed with tailless myosin V-HMM ($K'_{1D}k'_{+2D}$ = 42 $\mu M^{-1}\ s^{-1}$ in the absence of calcium and 148 $\mu M^{-1}\ s^{-1}$ in the presence of calcium) (Fig. 5, Table 1, and Scheme 2). Therefore, regulation of ADP binding by calcium presumably arises from binding to the associated calmodulin light chains and subsequent calcium-dependent changes in conformation and binding modes (6–9, 39), although contributions from cation binding to sites on myosin and/or actin filaments cannot be eliminated as a possible source. The observation that ADP binding is more rapid to tailless myosin V than myosin Va under all conditions examined suggests that the tail domain interacts with and modulates the biochemical properties of the motor even in the presence of calcium, as would be expected for a reversible calcium-dependent equilibrium.

Intramolecular Allostery and Strain Regulate ADP but Not ATP Binding to Actomyosin Va—With both heads strongly bound to actin, ADP binding, but not ATP binding, to recombinant tailless myosin V-HMM is accelerated relative to recombinant single-headed myosin V-S1 (19). ADP binding to HMM is favored largely by a ~5-fold tighter collision complex affinity compared with S1 (K'_{1D} = 14 μM for HMM and 74 μM for S1); the isomerization rate constant ($k'_{+2D} + k'_{-2D}$ = 589 s^{-1} for HMM and 973 s^{-1} for S1) is slightly reduced (Table 1 and Scheme 2).

Identical behavior was observed with recombinant, double-headed myosin VI (15), although ATP binding to actomyosin VI was also favored when both heads were strongly bound to actin, but to a lesser extent than ADP. It was proposed (15) that intramolecular stress generated when both heads bind strongly to actin strains the molecule and mediates opening of the myosin VI-HMM nucleotide binding cleft, which allows for more efficient nucleotide binding. A similar intramolecular strain-sensitive mechanism presumably accounts for the more rapid kinetics and tighter affinity of ADP binding to myosin V-HMM, although it will not be mediated through the class VI-specific insert, as proposed for myosin VI (15, 40, 41). The fact that intramolecular strain promotes ATP binding to actomyosin VI but not actomyosin V suggests that the myosin VI-specific insert is largely responsible for slow ATP binding (15, 40). The observed stress-dependent modulation of ADP binding kinetics and affinity is consistent with an ADP-linked conformational rearrangement of actomyosin V (14, 19, 42).

Implications for Processive Motility and Cargo Transport—In the presence of millimolar ATP and absence of calcium, myosin Va walks processively along an actin filament (3, 12, 13, 28, 29). The addition of ATP to myosin Va (and recombinant tailless myosin V-HMM) with both heads strongly bound to actin (at a density of 0.1–0.2 heads/actin subunit) increases the pyrene fluorescence, indicating population of the weak actin binding states, consistent with models in which myosin V does not dwell with both heads strongly bound to actin during a processive run at physiological [ATP] (43, 46). If myosin Va dwelled predominantly with both heads strongly bound to actin during a processive run, no net change in pyrene fluorescence would be observed upon the addition of ATP. The ^{18}O exchange anal-

ysis and mant-product release time courses (Fig. 6) are consistent with P_i release being very rapid upon actin encounter and during steady-state cycling, suggesting that the weakly bound or detached head, presumably the leading head during a processive run, has bound ADP (25, 29, 44, 45) but cannot bind actin strongly because it is restrained by the strongly bound trailing head (29, 43–46).

Time courses of fluorescence enhancement after mixing ATP with pyrene actomyosin Va are biphasic (Fig. 4*A*). We interpret the slow phase observed to reflect the population of myosin Va molecules that release both heads from actin and terminate a processive run, which modeling of processive run lengths (28) suggests occurs with a similar rate constant of 1–2 s^{-1}. The observation that the fast phase amplitude is larger than that of the slow phase implies that some double-headed detachment occurs with rapid ATP binding and that a fraction of the myosin V molecules initially bound strongly to actin with both heads are not processive.

We expect that cargo binding would disrupt the interaction between the tail domain and the motor domain, similar to the effect of calcium, and would enable both heads to bind actin and allow for efficient processive stepping. Release of cargo would permit the head-tail interaction to occur and cause myosin Va·ADP to bind actin strongly with only one head. In the presence of ATP, this head will dissociate from actin and rapidly rebind actin at a different location. Collectively, our results favor a mechanism in which myosin V detaches from actin after it releases bound cargo and rebinds actin at a different region of the cell once new cargo binds.

In addition to favoring formation of the extended conformation, calcium accelerates ADP binding to actomyosin Va independent of the tail domain (Fig. 5). This aspect of calcium regulation cannot be mimicked by cargo binding and may arise from changes in the mechanical properties of the regulatory neck domain and associated light chains. In the presence of calcium, the rate constant for ADP binding to tailless myosin Va is >100 times more rapid than that of ATP (Table 1 and Scheme 2). Therefore, ADP will bind over ATP with high probability even at very low [ADP]/[ATP] ratios, and would cause myosin Va to stall or terminate (28) a processive run. In either case, calcium is expected to decrease the effective processivity and run length of myosin Va.

Acknowledgments—We thank Drs. Peter Knight and Jim Sellers for freely communicating unpublished results.

REFERENCES

1. Reck-Peterson, S. L., Provance, D. W., Jr., Mooseker, M. S., and Mercer, J. A. (2000) *Biochim. Biophys. Acta* **1496,** 36–51
2. Krendel, M., and Mooseker, M. S. (2005) *Physiology* (*Bethesda*) **20,** 239–251
3. Mehta, A. D., Rock, R. S., Rief, M., Spudich, J. A., Mooseker, M. S., and Cheney, R. E. (1999) *Nature* **400,** 590–593
4. Reck-Peterson, S. L., Tyska, M. J., Novick, P. J., and Mooseker, M. S. (2001) *J. Cell Biol.* **153,** 1121–1126
5. Cheney, R. E., O'Shea, M. K., Heuser, J. E., Coelho, M. V., Wolenski, J. S., Espreafico, E. M., Forscher, P., Larson, R. E., and Mooseker, M. S. (1993) *Cell* **75,** 13–23
6. Cameron, L. C., Carvalho, R. N., Araujo, J. R., Santos, A. C., Tauhata, S. B., Larson, R. E., and Sorenson, M. M. (1998) *Arch. Biochem. Biophys.* **355,** 35–42
7. Wang, F., Thirumurugan, K., Stafford, W. F., Hammer, J. A., III, Knight, P. J., and Sellers, J. R. (2004) *J. Biol. Chem.* **279,** 2333–2336
8. Krementsov, D. N., Krementsova, E. B., and Trybus, K. M. (2004) *J. Cell Biol.* **164,** 877–886
9. Li, X. D., Mabuchi, K., Ikebe, R., and Ikebe, M. (2004) *Biochem. Biophys. Res. Commun.* **315,** 538–545
10. Thirumurugan, K., Sakamoto, T., Hammer, J. A., III, Sellers, J. R., and Knight, P. J. (2006) *Nature* **442,** 212–215
11. Liu, J., Taylor, D. W., Krementsova, E. B., Trybus, K. M., and Taylor, K. A. (2006) *Nature* **442,** 208–211
12. Rief, M., Rock, R. S., Mehta, A. D., Mooseker, M. S., Cheney, R. E., and Spudich, J. A. (2000) *Proc. Natl. Acad. Sci. U. S. A.* **97,** 9482–9486
13. Veigel, C., Wang, F., Bartoo, M. L., Sellers, J. R., and Molloy, J. E. (2002) *Nat. Cell Biol.* **4,** 59–65
14. Hannemann, D. E., Cao, W., Olivares, A. O., Robblee, J. P., and De La Cruz, E. M. (2005) *Biochemistry* **44,** 8826–8840
15. Robblee, J. P., Olivares, A. O., and De La Cruz, E. M. (2004) *J. Biol. Chem.* **279,** 38608–38617
16. Cheney, R. E. (1998) *Methods Enzymol.* **298,** 3–18
17. Rock, R. S., Rice, S. E., Wells, A. L., Purcell, T. J., Spudich, J. A., and Sweeney, H. L. (2001) *Proc. Natl. Acad. Sci. U. S. A.* **98,** 13655–13659
18. De La Cruz, E. M. (2005) *J. Mol. Biol.* **346,** 557–564
19. Robblee, J. P., Cao, W., Henn, A., Hannemann, D. E., and De La Cruz, E. M. (2005) *Biochemistry* **44,** 10238–10249
20. De La Cruz, E. M., Sweeney, H. L., and Ostap, E. M. (2000) *Biophys. J.* **79,** 1524–1529
21. Hackney, D. D. (2005) *Proc. Natl. Acad. Sci. U. S. A.* **102,** 18338–18343
22. Tauhata, S. B., dos Santos, D. V., Taylor, E. W., Mooseker, M. S., and Larson, R. E. (2001) *J. Biol. Chem.* **276,** 39812–39818
23. Geeves, M. A., Goody, R. S., and Gutfreund, H. (1984) *J. Muscle Res. Cell Motil.* **5,** 351–361
24. Nyitrai, M., Szent-Gyorgyi, A. G., and Geeves, M. A. (2003) *Biochem. J.* **370,** 839–848
25. Rosenfeld, S. S., and Sweeney, H. L. (2004) *J. Biol. Chem.* **279,** 40100–40111
26. Nyitrai, M., Szent-Gyorgyi, A. G., and Geeves, M. A. (2002) *Biochem. J.* **365,** 19–30
27. De La Cruz, E. M., Wells, A. L., Rosenfeld, S. S., Ostap, E. M., and Sweeney, H. L. (1999) *Proc. Natl. Acad. Sci. U. S. A.* **96,** 13726–13731
28. Baker, J. E., Krementsova, E. B., Kennedy, G. G., Armstrong, A., Trybus, K. M., and Warshaw, D. M. (2004) *Proc. Natl. Acad. Sci. U. S. A.* **101,** 5542–5546
29. Uemura, S., Higuchi, H., Olivares, A. O., De La Cruz, E. M., and Ishiwata, S. (2004) *Nat. Struct. Mol. Biol.* **11,** 877–883
30. Webb, M. R., Hibberd, M. G., Goldman, Y. E., and Trentham, D. R. (1986) *J. Biol. Chem.* **261,** 15557–15564
31. Sleep, J. A., Hackney, D. D., and Boyer, P. D. (1980) *J. Biol. Chem.* **255,** 4094–4099
32. Sleep, J. A., Hackney, D. D., and Boyer, P. D. (1978) *J. Biol. Chem.* **253,** 5235–5238
33. Hackney, D. D., and Clark, P. K. (1984) *Proc. Natl. Acad. Sci. U. S. A.* **81,** 5345–5349
34. De La Cruz, E. M., Wells, A. L., Sweeney, H. L., and Ostap, E. M. (2000) *Biochemistry* **39,** 14196–14202
35. Yengo, C. M., and Sweeney, H. L. (2004) *Biochemistry* **43,** 2605–2612
36. Nascimento, A. A., Cheney, R. E., Tauhata, S. B., Larson, R. E., and Mooseker, M. S. (1996) *J. Biol. Chem.* **271,** 17561–17569
37. Nyitrai, M., and Geeves, M. A. (2004) *Philos. Trans. R. Soc. Lond. B Biol. Sci.* **359,** 1867–1877
38. Prochniewicz, E., Walseth, T. F., and Thomas, D. D. (2004) *Biochemistry* **43,** 10642–10652
39. Martin, S. R., and Bayley, P. M. (2004) *FEBS Lett.* **567,** 166–170
40. Menetrey, J., Bahloul, A., Wells, A. L., Yengo, C. M., Morris, C. A., Sweeney, H. L., and Houdusse, A. (2005) *Nature* **435,** 779–785
41. Wells, A. L., Lin, A. W., Chen, L. Q., Safer, D., Cain, S. M., Hasson, T., Carragher, B. O., Milligan, R. A., and Sweeney, H. L. (1999) *Nature* **401,**

505–508
42. Volkmann, N., Liu, H., Hazelwood, L., Krementsova, E. B., Lowey, S., Trybus, K. M., and Hanein, D. (2005) *Mol. Cell* **19,** 595–605
43. De La Cruz, E. M., Ostap, E. M., and Sweeney, H. L. (2001) *J. Biol. Chem.* **276,** 32373–32381
44. Purcell, T. J., Sweeney, H. L., and Spudich, J. A. (2005) *Proc. Natl. Acad. Sci. U. S. A.* **102,** 13873–13878
45. Olivares, A. O., and De La Cruz, E. M. (2005) *Proc. Natl. Acad. Sci. U. S. A.* **102,** 13719–13720
46. De La Cruz, E. M., and Ostap, E. M. (2004) *Curr. Opin. Cell Biol.* **16,** 61–67
47. Stafford, W. F., Jacobsen, M. P., Woodhead, J., Craig, R., O'Neall-Hennessey, E., and Szent-Gyorgyi, A. G. (2001) *J. Mol. Biol.* **307,** 137–147